WORLD JOURNAL OF PHARMACEUTICAL RESEARCH
SJIF Impact Factor 8.074
Volume 7, Issue 7, 336-350. Conference Article SSN 2277–7105

SYNTHESIS, LUMINESCENCE, AND ELECTROCHEMICAL STUDIES OF DIOXADIAZA- MACROCYCLE AND EXTRACTION OF TOXIC METALS

Lynda Merlin D.*

Department of Chemistry, University College of Engineering, Kanchipuram, India.

Article Received on
13 Feb. 2018,
Revised on 06 March 2018,
Accepted on 27 March 2018
DOI: 10.20959/wjpr20187-11687

***Corresponding Author**
Lynda Merlin D.
Department of Chemistry, University College of Engineering, Kanchipuram, India.

ABSTRACT

The synthesis and photophysical and electrochemical properties of dioxadiaza macrocycle are reported. The 16-membered dioxadiaza macrocycle, 5,6,14,15-dibenzo-1,4-dioxa-8,12-diazacyclopentadeca-5,14-diene (**L1**) is synthesized by the Schiff base condensation of 1,4-bis(2′-formylphenyl)-1,4-dioxabutane (**1**) with 1,3-diaminopropane in dry ethanol followed by the in situ reduction of the Schiff base macrocycles using sodium borohydride and borax and characterized by single-crystal X-ray diffraction: triclinic, *P*-1. The free ligands **L1** emit in the visible region at 691 nm upon excitation in the UV region at 262 nm. The complexation of these macrocycles with these toxic metal ions is robust and leads to a large shift in emission maxima depending on the nature of the metal ion. The efficient complexation of these metal ions by the macrocycle **L1** could be exploited for the removal of these metal ions from the environmental samples. The ligand systems **L1** could serve as potential photochemical chemosensors for Cd(II), Hg(II), and Pb(II) as they are able to bind with these metal ions, and at the same time, signal their presence in fluid solution by the chelation enhanced fluorescence effect.

KEY WORDS: Macrocycles, Toxic metals, Heavy metals.

INTRODUCTION

Macrocyclic ligands are used as selective complexants of metal ions[1] for the treatment of metal intoxication,[2] in radioactive wastewater treatment,[3] as functional groups for chelating ion exchange materials, selective metal extractants in hydrometallurgy,[4] corrosion inhibitor,[5] solar cell functional materials,[6] gas sensors,[7] and in nonlinear optical devices.[8]

The selective binding of certain metals with macrocycles is exploited as models for active sites in metalloenzymes[9] and protein-metal binding sites in biological systems,[10] for the selective uptake and transport of metal ions[11] and oxygen[12] in biological systems,[13] and in radioactive diagnosis and treatment.[14]

Several classes of macrocyclic ligands such as polyaza macrocycles, Schiff base macrocycles, oxazolidine-containing macrocycles, polyoxa macrocycles, polyoxaaza macrocycles, polyoxa- and polyoxaaza coronands, crown ethers, lariat crown ethers, cryptands, cavitands, calixarenes, carcerands, cyclodextrins, cryptophanes, cyclophanes, hemispherands, catenanes, podands, compartmental macrocyclic ligands which form homo- and heterodinuclear complexes, structurally reinforced macrocycles, redox-responsive macrocycles, photoresponsive macrocycles, pH-responsive macrocycles, chromogenic macrocycles, siderophores, sepulchrates, spherands, molecular clefts, bibracchial macrocycles, and macrocycles containing pendant arms have been reported. Macrocycles which contain varying combination of aza-, oxa-, phospha-, and sulpha ligating atoms can be tailored to accommodate specific metal ions by fine-tuning the ligand design features such as the macrocyclic hole size, nature of the ligand donors, donor set, donor array, ligand conjugation, ligand substitution, number and size of the chelate rings, ligand flexibility, and nature of the ligand backbone.

EXPERIMENTAL SECTION

3.1 Materials

3.1.1 Reagents

Salicylaldehyde, 1,2-dibromoethane, 1,3-dibromopropane, mesitylene, ethylenediamine, 1,3-diaminopropane, and *α,α'*-diamino-*m*-xylene (Fluka); *N*-bromo- succinimide, *p*-xylene, paraformaldehyde, potassium bromide, acetic acid, sulphuric acid, sodium hydroxide, potassium carbonate, mercuric chloride, lead nitrate, sodium hydrogencarbonate, sodium metal, sodium chloride, calcium oxide, sodium borohydride, and borax (Merck), cadmium chloride, benzophenone, and benzoyl peroxide (S. D. Fine Chem Ltd); and silica gel (TLC, 100-120 mesh, ACME) were used as received. Molecular sieves 4Å (Aldrich) was used after activating by heating in an oven at 120 °C for 8 h. Calcium hydride (Aldrich) was used as such for the purification of the solvents. Calcium chloride (anhydrous) and sodium sulfate (anhydrous) (Merck, India) were used as such for drying solvents. Silica gel (blue indicator, Fluka), activated by heating in an oven at 150 °C overnight, was used as the desiccant.

3.2 Physical Measurements

3.2.1 Infrared spectra. Infrared spectra were recorded on a Perkin-Elmer spectrum RX-I FT-IR Spectrometer in the range of 4000-400 cm^{-1}. Spectra of the solid samples were recorded by making transparent KBr pellets. Potassium bromide (FT-IR grade, Fluka) was used to make the pellets. Nujol mull (Fluka) was used for liquid samples and spectra were recorded using NaCl windows.

3.2.2 Mass spectra. FAB mass spectra were recorded on a JEOL SX 102/DA-6000 Mass spectrometer/data system using argon/xenon (6 kV, 10 mA) as the FAB gas. The accelerating voltage was 10 kV and the spectra were recorded at room temperature. *m*-Nitrobenzyl alcohol (NBA) was used as the matrix. The matrix peaks appear at *m/z* 136, 137, 154, 289, and 307 in the absence of any metal ion. If metal ion such as Na^+ is present these peaks may be shifted accordingly. The electrospray mass spectra were recorded on a micromass Quattro II triple quadrupole mass spectrometer. The sample dissolved in suitable solvent such as methanol, acetonitrile, or water was introduced into the ESI source through a syringe pump at the rate of 5 μL per min. The ESI capillary was set at 3.5 kV and the cone voltage at 40 V. The average spectrum of 6-8 scans was printed. The MALDI-TOF mass spectra were run a Micromass TofSpec 2E instrument using a nitrogen 337 nm laser (4 ns pulse). Atleast 40-50 shots were summed up. The matrix used was 2,5-dihydroxy benzoic acid and α-cyanohydroxy cinnamic acid dissolved in chloroform and acetonitrile/methanol. The sample and the matrix were spotted on the MALDI target and allowed to dry before introducing into the mass spectrometer.

3.2.3 CHN analysis. CHN microanalyses were carried out using a Perkin-Elmer 2400 Series II CHNS/O Elemental Analyzer interfaced with a Perkin-Elmer AD 6 Autobalance. Helium was used as the carrier gas.

3.2.4 Electronic absorption spectra. The electronic absorption spectra were recorded on a Perkin-Elmer Lambda 25 UV-Visible spectrophotometer controlled by the WinLab software through computer. The spectra were recorded in the region 190-900 nm in chloroform and *N*,*N*-dimethylformamide at 25 ºC using a matched pair of Teflon stoppered quartz cell of path length 1 cm. Solvent corrections were carried out before recording the spectra.

3.2.5 Fluorescence spectra. Fluorescence spectra were recorded on a Perkin-Elmer LS-55 Luminescence Spectrometer. The excitation source was a 150 W CW Xenon lamp. The

band pass for the excitation and emission monochromator was set at 5 nm. Quartz cell of 0.5 cm path length was used.

3.2.6 Electrochemical studies. Electrochemical studies were performed on a EG&G PAR 273A Potentiostat/Galvanostat. The cyclic voltammograms were recorded using RDE0018 Analytical Cell Kit consisting of a thermostated cell bottom, working electrode, platinum counter electrode, and Ag/Ag^{+} reference electrode. The auxiliary electrode was connected to the test solution through the counter electrode bridge tube. The reference electrode was separated from the test solution through the bridge tube containing AgCl-KCl filling solution. The cyclic voltammograms were recorded on a gold disk milli electrode and/or dropping mercury electrode EG&G PAR 303A SMDE using a $\sim 10^{-3}$ M solution of the complex in acetate buffer. Acetate buffer (pH = 4.5) was prepared by mixing sodium acetate (0.1 M) and acetic acid (0.1 M). Oxygen free argon, saturated with the solvent vapor, was flushed through each sample solution through the purge tube assembly for 30 min before voltammetry was performed and all measurements were carried out in an atmosphere of argon at 25 ºC. All operations were performed through the computer using EG&G Model 270 software and all electrochemical calculations were carried out using the EG&G Power Suite software.

3.2.7 NMR spectra. ^{1}H NMR spectra were recorded on a Jeol GSX-400 multinuclear NMR spectrometer working at 400 MHz at 25 ºC. Spectra were recorded in $CDCl_3$ (100 atom % D), CD_3CN (99.9 atom % D), or DMSO-d_6 (99.9 atom % D) (Aldrich). The ^{13}C NMR spectra were recorded at 100 MHz using Jeol GSX-400 instrument. The standard 5 mm probe was used for ^{1}H and ^{13}C NMR measurements.

3.2.8 Rotavapor. Buchi rotavapor (Model R-124) was used to remove the solvent and isolate the products at low temperature and pressure.

3.2.9 Cryostat. Heto Holton cryogenic circulator bath (- 45 ºC) was used to carry out the reactions at low temperature. The circulating bath was filled with water-ethylene glycol (3:2 v/v) for bath temperature of -10 ºC and pure methanol for - 45 ºC.

3.2.10 X-ray diffraction. The single crystal X-ray diffraction was carried out using an Enraf Nonius CAD4 X-ray diffractometer, equipped with graphite monochromator and the radiation source was Cu*K*α. The unit cell parameters were determined by the method of short vectors using 25 reflections collected by search routine from different zones of the crystal.

The intensity data were gathered using ω-2θ scan technique. SIR92 program was used to solve the crystal structure. The structure was refined using the software SHELXL97. ORTEP32 in WinGX software package was used for the molecular graphics.

3.4.2 5,6,14,15-Dibenzo-1,4-dioxa-8,12-diazacyclopentadeca-5,14-diene (6). Compound **6** was synthesised by the procedure reported by Adam et al.[243b] 1,3-Diaminopropane (1.66 mL, 20 mmol) in absolute ethanol (80 mL) was added to a solution of 1,4-bis(2′-formylphenyl)-1,4-dioxabutane (5.40 g, 20 mmol) in absolute ethanol (300 mL), refluxed for 4 h, and cooled to room temperature. Sodium borohydride (2.96 g, 80 mmol) and a few milligram of borax were added and stirred for 1 h. The excess sodium borohydride was quenched with water and the reaction mixture was extracted with 2 x 200 mL portions of chloroform. The organic layer was dried over anhydrous sodium sulfate, filtered, concentrated to 20 mL in a rotavapor, and added to 100 mL of ether under stirring. The white precipitate that separated out was filtered and dried in vacuum. Crystals suitable for the X-ray diffraction were obtained by slow evaporation of a solution of **6** in methanol in the presence of a trace amount of sodium nitrate for 30 days. Yield (6.14 g, 85.6%), mp 127 °C. Analytical calculated for $C_{19}N_2O_2H_{24}$: C 73.04, H 7.74, N 8.96. Found: C 73.02, H 7.67, N 8.84. IR (KBr, cm^{-1}): 3295.9 ν(N-H); 3035.7 ν_s(C-H) and 752.8 δ(C-H) (aromatic); 2913.3 ν_{as}(C-H), 2806.9 ν_s(C-H) (aliphatic); 1599.8, 1493.1, and 1452.1 ν_s(C=C) (aromatic); 1244.3 ν_{as}(C-O-C); 976.5 ω(CH_2), 942.1 τ(CH_2), and 881.8 ρ(CH_2) (methylene). FAB MS: *m/z* 313 $[M]^+$, 268 $[M-(C_3H_{10})]^+$. ^{1}H NMR ($CDCl_3$, 298 K): δ 1.17 (2 H, p, *J* = 5.7 Hz, NH-CH_2-C*H*$_2$-CH_2-NH), 1.74 (2 H, s, N-*H*), 2.63 (4 H, t, *J* = 5.6 Hz, NH-C*H*$_2$-CH_2-C*H*$_2$-NH), 3.74 (4 H, s, Ar-C*H*$_2$-NH), 4.36 (4 H, s, OC*H*$_2$-C*H*$_2$O), 6.88 (2 H, t, *J* = 6 Hz, Ar*H*$_f$), 6.92 (2 H, d, *J* = 7.3 Hz, Ar*H*$_g$), 7.2 (2 H, d, *J* = 7.3 Hz, Ar*H*$_h$), 7.26 (2 H, t, *J* = 7.5 Hz, Ar*H*$_i$). ^{13}C NMR ($CDCl_3$, 298 K): δ 29.2, 47.4, 51.6, 65.9, 110.3, 120.8, 128.1, 128.8, 131.4, 157.1.

4.1.5 Synthesis of 1,4-bis(2′-formylphenyl)-1,4-dioxabutane (3)

O-Alkylation of salicylaldehyde (1 equiv) with dibromoethane (1 equiv) (Williamson's condensation) in the presence of sodium hydroxide (2 equiv) as the proton scavenger in water-ethanol medium gives **3** as white needles in 61% yield. The unreacted salicylaldehyde is removed by washing with water. The reaction is illustrated in Scheme 3.

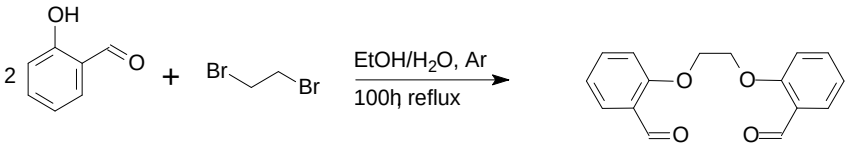

Scheme 3. Synthesis of 1,4-bis(2′-formylphenyl)-1,4-dioxabutane (3).

4.1.6 Characterization of 1,4-bis(2′-formylphenyl)-1,4-dioxabutane (3)

4.1.6.1 Infrared spectrum. The infrared spectrum of **3** shows absorption bands at 3076.1 and 753.8 cm^{-1} assignable to the aromatic ν_s(C-H) and δ(C-H) vibrations, respectively. The absorption bands at 2922.8 and 2866.0 cm^{-1} are assignable to the aliphatic ν_{as}(C-H) and ν_s(C-H) vibrations, respectively. The absorption band at 1652.2 cm^{-1} is assignable to the ν_s(C=O) vibration. The absorption bands at 1597.7, 1484.7, and 1452.0 cm^{-1} are assignable to the aromatic ν_s(C=C) vibration. The absorption band at 1248.7 cm^{-1} is assignable to the aromatic ν_{as}(C-O-C) vibration. The absorption bands at 944.5, 860.0, and 834.9 cm^{-1} are assignable to the ω(CH_2), τ(CH_2), and ρ(CH_2) vibrations, respectively, of the methylene groups.[89b]

4.1.6.2 FAB mass spectrum. The FAB mass spectrum of **3** shows the molecular ion peak at *m/z* 271 corresponding to the fragment $[M]^+$ $(C_{16}H_{14}O_4)^+$. The peak at *m/z* 149 is due to the fragment $[M\text{-}C_7H_6O_2]^+$ $(C_9H_8O_2)^+$. The peak at *m/z* 136 is assignable to the fragment $[M\text{-}(C_8H_6O_2)]^+$ $(C_8H_8O_2)^+$ formed by the loss of one methylene appended salicylaldehyde group from the molecular ion. The peak at *m/z* 121 is due to the fragment $(C_7H_5O_2)^+$ which corresponds to salicylaldehyde. The FAB mass spectrum of **3** is shown in Figure 4.6.

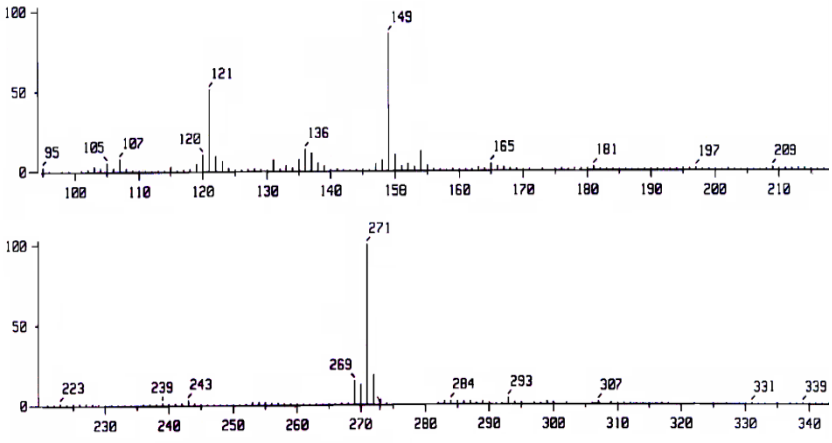

Figure 4.6. FAB mass spectrum of 1,4-bis(2′-formylphenyl)-1,4-dioxabutane (3).

4.2.3 Synthesis of 5,6,14,15-dibenzo-1,4-dioxa-8,12-diazacyclopentadeca-5,14-diene (6)

The Schiff base condensation of 1,4-bis(2′-formylphenyl)-1,4-dioxabutane (**3**) and 1,3-diaminopropane in dry ethanol followed by the in situ reduction of Schiff base macrocycle

with sodium borohydride and borax gives **6** as white precipitate in 85.6% yield. The reaction is depicted in Scheme 6.

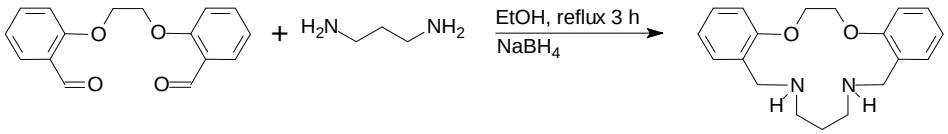

Scheme 6. Synthesis of 5,6,14,15-dibenzo-1,4-dioxa-8,12-diazacyclopentadeca-5,14-diene (6).

4.2.4 Characterization of 5,6,14,15-dibenzo-1,4-dioxa-8,12-diazacyclopenta-deca-5,14-diene (6)

4.2.4.1 Infrared spectrum. The infrared spectrum of **6** shows a strong absorption band at 3295.9 corresponding to the ν(N-H) vibration.[15] The absorption bands at 3035.7 and 752.8 cm^{-1} are assignable to the aromatic ν_s(C-H) and δ(C-H) vibrations, respectively. The absorption bands at 2913.3 and 2806.9 cm^{-1} are due to the aliphatic ν_{as}(C-H) and ν_s(C-H) vibrations, respectively. The absorption bands at 1599.8, 1493.1, and 1452.1 cm^{-1} are assignable to the aromatic ν_s(C=C) vibrations. The absorption band at 1244.3 cm^{-1} is assignable to the aromatic ν_{as}(C-O-C) vibration. The absorption bands at 976.5, 942.1, and 881.8 cm^{-1} are assignable to the ω(CH_2), τ(CH_2), and ρ(CH_2) vibrations, respectively, of the methylene groups.[15]

4.2.4.2 FAB mass spectrum. FAB mass spectrum of **6** shows a peak at *m/z* 313 corresponding to the molecular ion $[M]^+$ $(C_{19}N_2O_2H_{24})^+$. The peak at *m/z* 268 is attributed to the fragment $[M-(C_3H_{10})]^+$ $(C_{16}N_2O_2H_{14})^+$ formed by the loss of a propylene group from the macrocycle. The peak at *m/z* 121 is due to the salicylaldehyde moiety. The FAB mass spectrum of **6** is shown in Figure 4.12.

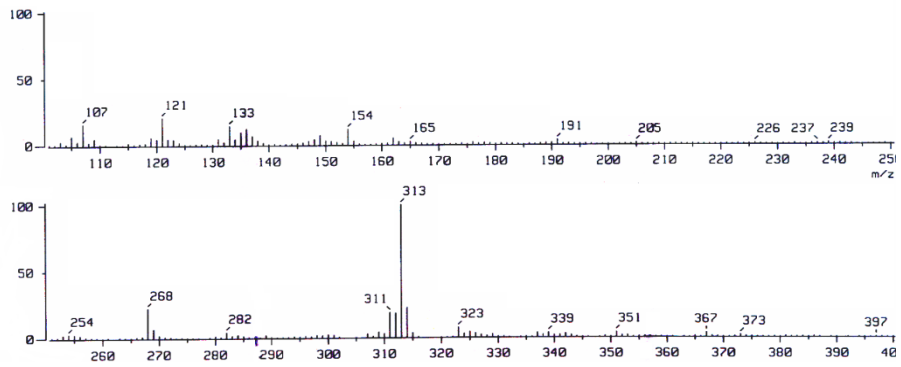

Figure 4.12. FAB mass spectrum of 5,6,14,15-dibenzo-1,4-dioxa-8,12-diazacyclopentadeca-5,14-diene (6).

4.2.4.3 ^{1}H NMR spectrum. The ^{1}H NMR spectrum of **6** in $CDCl_3$ consists of nine resonances due to the different types of protons. The signal at 1.17 ppm corresponds to the center methylene protons (NH-CH_2-CH_2-CH_2-NH) of the amine group. The singlet at 1.74 ppm corresponds to the secondary amine protons. The signal at 2.63 ppm corresponds to the aliphatic methylene protons (NH-CH_2-CH_2-CH_2-NH). The resonance at 3.74 ppm is attributed to the methylene protons (NH-CH_2-Ar) attached to the phenyl ring. The signal at 4.36 ppm corresponds to the aliphatic methylene protons (OCH_2-CH_2O) bonded to the oxygen atoms of the macrocycle. The aromatic protons ArH_f, ArH_g, ArH_h, and ArH_i resonate at 6.88, 6.92, 7.20, and 7.26 ppm, respectively. The ^{1}H NMR spectrum of **6** is shown in Figure 4.13.

4.2.4.4 ^{13}C NMR spectrum. The ^{13}C NMR spectrum of **6** displays ten different resonances. The signal at 29.29 ppm is due to the NH-CH_2-CH_2-CH_2-NH carbon of 1,3-diaminopropane. The resonance at 47.49 ppm is due to the NH-CH_2-CH_2-CH_2-NH carbon. The signal at 51.63 ppm corresponds to the methylene carbon (NH-CH_2-Ar) attached to the phenyl group. The resonance at 65.91 ppm is due to the (OCH_2-CH_2O) carbon. The signals at 110.33, 120.83, 128.13, 128.82, 131.43, and 157.17 ppm are due to the C_e-C_j carbons of the benzene ring. The ^{13}C NMR spectrum of **6** is shown in Figure 4.14.

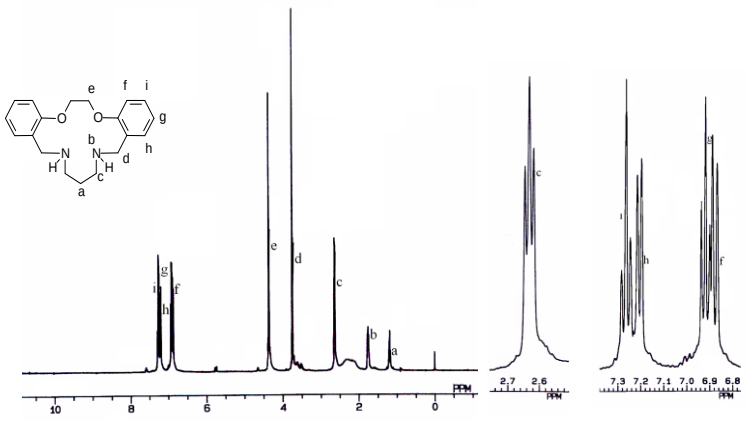

Figure 4.13. 400 MHz ^{1}H NMR spectrum of 5,6,14,15-dibenzo-1,4-dioxa-8,12-diazacyclopentadeca-5,14-diene (6) in $CDCl_3$.

4.2.4.5 Off-resonance decoupled ^{13}C NMR spectrum. The off-resonance decoupled spectrum of **6** shows a triplet for the CH_2 carbon, a doublet for the *CH* carbon and a singlet for the carbon without hydrogen. The off-resonance decoupled spectrum of **6** is shown in Figure 4.15.

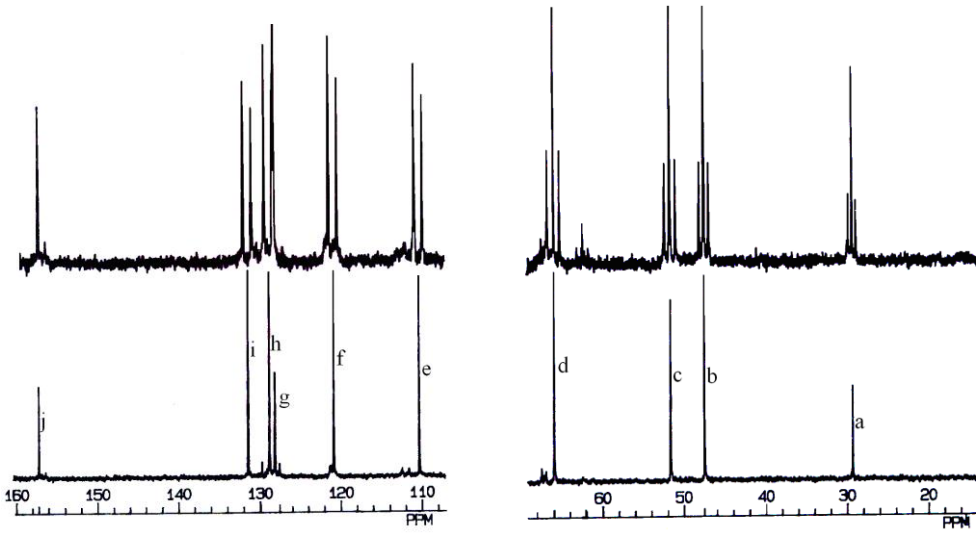

Figure 4.15. Off-resonance decoupled ^{13}C NMR spectrum of 5,6,14,15-dibenzo-1,4-dioxa-8,12-diaza -cyclopentadeca-5,14-diene (6) in $CDCl_3$.

4.2.4.6 Electronic absorption spectrum. The electronic absorption spectrum of **6** in chloroform at 25 °C shows three absorption bands at 274.27, 269.52, and 24.52 nm assignable to the n-π* and π-π* transitions.[89a] Electronic absorption spectrum of **6** is shown in Figure 4.16.

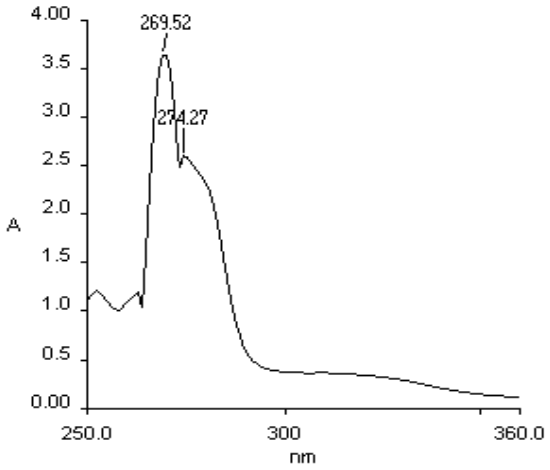

Figure 4.16. Electronic absorption spectrum of 5,6,14,15-dibenzo-1,4-dioxa-8,12-diazacyclopenta- deca-5,14-diene (6) in chloroform at room temperature.

4.2.4.8 XRD crystal structure of 6. Single crystal of **6** suitable for X-ray diffraction is obtained by recrystallization in methanol. The crystal data of **6** are given in Table 4.1 and 4.2. The ORTEP view of 6 is shown in Figure 4.17. The hydrogen bonding view of 6 is shown in Figure 4.18.

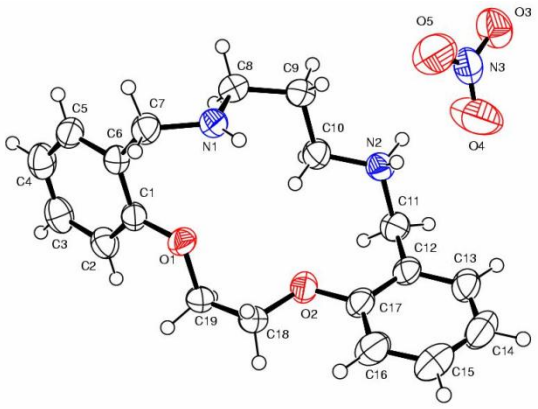

Figure 4.17. ORTEP view of 5,6,14,15-dibenzo-1,4-dioxa-8,12-diazacyclopentadeca-5,14-diene (6) (B. Brainard and V. Alexander, CCDC #708247, November 2008).

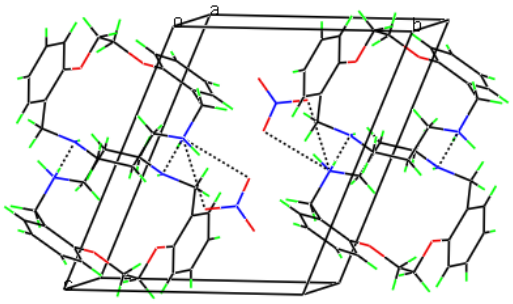

Figure 4.18. The hydrogen bonding structure of 5,6,14,15-dibenzo-1,4-dioxa-8,12-diazacyclo- pentadeca-5,14-diene (6).

Table 4.1. The crystal data of 5,6,14,15-dibenzo-1,4-dioxa-8,12-diazacyclopenta- deca-5,14-diene (6).

description	data
empirical formula	$C_{19}H_{25}N_3O_5$
formula weight	375.42
color	pale yellow
crystal description	plate
crystal size/mm	0.3 x 0.3 x 0.2
diffractometer	CAD4
radiation type	Cu $K\alpha$
crystal system	triclinic
space group	*P*-1
a/Å	9.4245(3)
b/Å	10.5720(4)
c/Å	10.9577(4)
α/deg	109.880(2)
β/deg	93.183(2)

γ/deg	111.059(2)
V/Å^3	938.29(6)
Z	2
ρ_{calcd}/g cm^{-3}	1.329
λ/Å	0.71073
T/K	293(2) K
absorption correction	ψ scan
absorption correction range	0.9808 to 0.9715
2θ range/deg	2.02-31.34
F(000)	400
no of reflns collected	23285
no of unique observed reflns	5997
no of parameters	252
goodness-of-fit on F^2	1.028
final R indices [I>2σ(I)]	R1 = 0.0575, wR2 = 0.1647
R indices, all data	R1 = 0.0954, wR2 = 0.2002
largest diff. peak and hole	0.600 and -0.516
absorption coefficient	0.097

Table 4.2. Bond lengths (Å) and angles (deg) for 5,6,14,15-dibenzo-1,4-dioxa-8,12-diazacyclopentadeca-5,14-diene (6).

Bond lengths (Å)		bond lengths (Å)	
N1-C8	1.459(2)	N1-C7	1.471(2)
N1-H1A	0.8600	N2-C10	1.481(2)
N2-C11	1.505(2)	N2-H2C	0.97(3)
N2-H2D	0.88(3)	N3-O4	1.217(3)
N3-O3	1.230(2)	N3-O5	1.233(3)
O1-C1	1.3706(19)	O1-C19	1.4279(19)
O2-C17	1.369(2)	O2-C18	1.426(2)
C1-C2	1.386(2)	C1-C6	1.400(2)
C2-C3	1.388(3)	C2-H2B	0.9300
C3-C4	1.368(3)	C3-H3A	0.9300
C4-C5	1.382(3)	C4-H4A	0.9300
C5-C6	1.387(2)	C5-H5A	0.9300
C6-C7	1.508(2)	C7-H7A	0.9700
C7-H7B	0.9700	C8-C9	1.521(3)
C8-H8A	0.9700	C8-H8B	0.9700
C9-C10	1.517(2)	C9-H9A	0.9700
C9-H9B	0.9700	C10-H10A	0.9700
C10-H10B	0.9700	C11-C12	1.497(3)
C11-H11A	0.9700	C11-H11B	0.9700
C12-C13	1.390(2)	C12-C17	1.396(2)
C13-C14	1.375(3)	C13-H13A	0.9300

C14-C15	1.365(4)	C14-H14A	0.9300
C15-C16	1.373(3)	C15-H15A	0.9300
C16-C17	1.389(3)	C16-H16A	0.9300
C18-C19	1.492(3)	C18-H18A	0.9700
C18-H18B	0.9700	C19-H19A	0.9700
C19-H19B	0.9700	-	-

Bond angles (deg)		**bond angles (deg)**	
C8-N1-C7	114.53(15)	C8-N1-H1A	122.7
C7-N1-H1A	122.7	C10-N2-C11	113.66(14)
C10-N2-H2C	112.0(15)	C11-N2-H2C	108.7(15)
C10-N2-H2D	113.9(16)	C11-N2-H2D	106.7(16)
H2C-N2-H2D	101(2)	O4-N3-O3	122.5(2)
O4-N3-O5	117.0(2)	O3-N3-O5	120.2(2)
C1-O1-C19	117.95(13)	C17-O2-C18	118.11(14)
O1-C1-C2	123.96(15)	O1-C1-C6	115.49(14)
C2-C1-C6	120.55(16)	C1-C2-C3	119.63(18)
C1-C2-H2B	120.2	C3-C2-H2B	120.2
C4-C3-C2	120.64(18)	C4-C3-H3A	119.7
C2-C3-H3A	119.7	C3-C4-C5	119.49(18)
C3-C4-H4A	120.3	C5-C4-H4A	120.3
C4-C5-C6	121.70(18)	C4-C5-H5A	119.1
C6-C5-H5A	119.1	C5-C6-C1	117.95(16)
C5-C6-C7	120.64(16)	C1-C6-C7	121.31(15)
N1-C7-C6	116.14(13)	N1-C7-H7A	108.3
C6-C7-H7A	108.3	N1-C7-H7B	108.3
C6-C7-H7B	108.3	H7A-C7-H7B	107.4
N1-C8-C9	110.46(15)	N1-C8-H8A	109.6
C9-C8-H8A	109.6	N1-C8-H8B	109.6
C9-C8-H8B	109.6	H8A-C8-H8B	108.1
C10-C9-C8	110.68(15)	C10-C9-H9A	109.5
C8-C9-H9A	109.5	C10-C9-H9B	109.5
C8-C9-H9B	109.5	H9A-C9-H9B	108.1
N2-C10-C9	113.21(15)	N2-C10-H10A	108.9
C9-C10-H10A	108.9	N2-C10-H10B	108.9
C9-C10-H10B	108.9	H10A-C10-H10B	107.7
C12-C11-N2	113.24(14)	C12-C11-H11A	108.9
N2-C11-H11A	108.9	C12-C11-H11B	108.9
N2-C11-H11B	108.9	H11A-C11-H11B	107.7
C13-C12-C17	117.64(18)	C13-C12-C11	120.45(17)
C17-C12-C11	121.87(16)	C14-C13-C12	122.1(2)
C14-C13-H13A	118.9	C12-C13-H13A	118.9
C15-C14-C13	118.99(19)	C15-C14-H14A	120.5
C13-C14-H14A	120.5	C14-C15-C16	121.2(2)
C14-C15-H15A	119.4	C16-C15-H15A	119.4
C15-C16-C17	119.8(2)	C15-C16-H16A	120.1
C17-C16-H16A	120.1	O2-C17-C16	123.70(17)
O2-C17-C12	115.98(15)	C16-C17-C12	120.32(17)

O2-C18-C19	108.12(14)	O2-C18-H18A	110.1
C19-C18-H18A	110.1	O2-C18-H18B	110.1
C19-C18-H18B	110.1	H18A-C18-H18B	108.4
O1-C19-C18	108.02(14)	O1-C19-H19A	110.1
C18-C19-H19A	110.1	O1-C19-H19B	110.1
C18-C19-H19B	110.1	H19A-C19-H19B	108.4

CONCLUSIONS

The dioxadiaza macrocycle 5,6,14,15-dibenzo-1,4-dioxa-8,12-diazacyclopentadeca-5,14-diene (**6**) The macrocycle **6** is characterized by CHN analysis, IR, ^{1}H and ^{13}C NMR spectra, FAB mass spectrum, and single crystal X-ray diffraction and the macrocycle The presence of basic amino sites in macrocycles enables the formation of protonated macrocyclic moieties, which can interact with inorganic and organic anions. By reactions with some anionic and neutral organic and biological substrates supramolecular assemblies can be developed with specific properties and applications. Thus, very efficient new separation methodologies could be developed on the basis of the parameters influencing the dynamic complexation and decomplexation of specific ionic or neutral species with these host ligand systems. The search for macrocyclic systems which are able to selectively recognize transition and heavy metal ions remains a topic of current interest. The free macrocycles and the complexes are luminescent at room temperature in fluid solution.

REFERENCES

1. (a) Blain, S.; Appriou, P.; Chaumeil, H.; Handel, H. *Anal. Chim. Acta* 1990; *232:* 331. (b) Tsubuke, H.; Yoden, T.; Iwachido, T.; Zenki, M. *J. Chem. Soc., Chem. Commun*. 1991, 1069. (c) Handel, H.; Muller, R. F.; Guglielmetti, R. *Helv. Chim. Acta* 1983; 66: 514.
2. (a) Bullman, R. A. *Struct. Bonding* 1987; *67:* 91. (b) Bryce-Smith, D. *Chem. Soc. Rev*. 1986; *15:* 93.
3. Sahni, S. K.; Reedijk, J. *Coord. Chem. Rev*. 1984; *59:* 1.
4. Green, B. R.; Hancock, R. D. *J. S. Afr. Inst. Min. Metall*. 1982; *82:* 303.
5. Beltran, H. I.; Esquivel, R.; Sosa-Sanchez, A.; Sosa-Sanchez, J. L.; Hopfl, H.; Barba, V.; Farfan, N.; Garcia, M. G.; Xometl, O. O.; Rivera, L. S. Z. *Inorg. Chem*. 2004; *43:* 3555.
6. (a) Wohrle, D.; Meissner, D. *Adv. Mater*. 1991, *3*, 129. (b) Eichhorn, H. *Porphyrins and Phthalocyanines* 2000; *4:* 88.
7. Wright, J. D. *Prog. Surf. Sci*. 1989; *31:* 1.
8. (a) Nalwa, H. S.; Shirk, J. S. In *Phthalocyanines: Properties and Applications*; Leznoff, C. C., Lever, A. B. P. Eds. VCH; 1996; p 79. (b) Shirk, J. S.; Pong, R. G. S.; Flom, S. R.;

Heckmann, H.; Hanack, M. *J. Phys. Chem. A* 2000; *104:* 1438. (c) de la Torre, G.; Vazquez, P.; Agullo-Lopez, F.; Torres, T. *J. Mater. Chem*. 1998; *8:* 1671.

9. (a) Clewley, R. G.; Slebocka-Tilk, H.; Brown, R. S. *Inorg. Chim. Acta* 1987; *157:* 233. (b) Read, R. J.; James, M. N. G. *J. Am. Chem. Soc*. 1981; *103:* 6947. (c) Kimura, E.; Shiota, T.; Koike, T.; Shiro, M.; Kodama, M. *J. Am. Chem. Soc*. 1990; *112:* 5805. (d) Norman, P. R. *Inorg. Chim. Acta* 1987; *130:* 1. (e) Gellman, S. H.; Petter, R.; Breslow, R. *J. Am. Chem. Soc*. 1986; *108:* 2388. (f) Breslow, R.; Berger, D.; Huang, D. L. *J. Am. Chem. Soc*. 1990; *112:* 3686. (g) Mochizuki, K.; Manaka, S.; Takeda, I.; Kondo, T. *Inorg. Chem*. 1996; *35:* 5132. (h) Bencini, A.; Bianchi, A.; Paoletti, P.; Paoli, P. *Pure Appl. Chem*. 1993; *65*: 381. (i) Wieghardt, K. *Angew. Chem., Int. Ed. Engl*. 1989; *28;* 1153. (j) Tolman, W. B. *Acc. Chem. Res*. 1997; *30:* 227.
10. (a) Kimura, E. *Pure Appl. Chem*. 1993; *65:* 355. (b) *Environmental Inorganic Chemistry*; Martell, A. E., Irgolic, K. J., Eds.; VCH Publishers: Deerfield Beach, FL, 1985. (c) Horrocks, W. DeW., Jr.; Albin, M. *Prog. Inorg. Chem*. 1984; *31:* 1.
11. Kimura, E.; Dalimunte, C. A.; Yamashita, A.; Machida, R. *J. Chem. Soc. Chem. Commun*. 1985; 1041.
12. (a) Kimura, E.; Sasada, M.; Shionoya, M.; Koike, T.; Kurosaki, H.; Shiro, M. *J. Bioinorg. Chem*. 1997; *2:* 74. (b) Kimura, E.; Machida, R.; Kodama, M. *J. Am. Chem. Soc*. 1984; *106:* 5497. (c) Kimura, E.; Machida, R. *J. Chem. Soc., Chem. Commun*. 1984; 499. (d) Kimura, E.; Shionoya, M.; Mita, T.; Litaka, Y. *J. Chem. Soc., Chem. Commun*. 1987; 1712.
13. Kimura, E.; Kurogi, Y.; Takahashi, T. *Inorg. Chem*. 1991; *30:* 4117.
14. (a) Reichert, D. E.; Lewis, J. S.; Anderson, C. J. *Coord. Chem. Rev*. 1999; *184:* 3. (b) Thunus, L.; Lejeune, R. *Coord. Chem. Rev*. 1999, *184*, 125. (c) Volkert, W. A.; Hoffman, T. J. *Chem. Rev*. 1999; *99:* 2269. (d) Chappell, L. L.; Dadachova, E.; Milenic, D. E.; Garmestani, K.; Wu, C.; Brechbiel, M. W. *Nucl. Med. Biol*. 2000; *27:* 93. (e) Milenic, D. E.; Garmestani, K.; Chappell, L. L.; Dadachova, E.; Yordanov, A.; Schlom, J. Ma. D.; Brechbiel, M. W. *Nucl. Med. Biol*. 2002; *29;* 431. (f) Hu, F.; Cutler, C. S.; Hoffman, T.; Sieckman, G.; Volkert, W. A.; Jurisson, S. S. *Nucl. Med. Biol*. 2002; *29:* 423.
15. (a) Vicente, M.; Bastida, R.; Macias, A.; Valencia, L.; Geraldes, C. F. G. C.; Brondino, C. D. *Inorg. Chim. Acta* 2005; *358:* 1141. (b) Bozic, L. T.; Visnjevac, A.; Marotta, E.; Prodic, B. K. *Polyhedron* 2005; *24:* 97. (c) Takafuji, M.; Ide, S.; Ihara, H.; Xu, Z. *Chem. Mater*. 2004; *16:* 1977. (d) Suresh Kumar, D.; Alexander, V. *Polyhedron* 1999; *18:* 1561. (e) Suresh Kumar, D.; Arul Joseph Aruna, V.; Alexander, V. *Polyhedron* 1999; *18:* 3123.

(f) Suresh Kumar, D.; Alexander, V. *Inorg. Chim. Acta* 1995; *238:* 63. (g) Nakamoto, K. *Infrared and Raman Spectra of Inorganic and Coordinartion Compounds*; Part B, 5th ed.; Wiley-Interscience: New York, 1997.